Equation of State of Cold Quark Matter to $O(\alpha_s^3 \ln \alpha_s)$

Tyler Gorda,[1,2,*] Risto Paatelainen,[3,†] Saga Säppi,[4,5,‡] and Kaapo Seppänen[3,§]
[1]*Technische Universität Darmstadt, Department of Physics, 64289 Darmstadt, Germany*
[2]*ExtreMe Matter Institute EMMI, GSI Helmholtzzentrum für Schwerionenforschung GmbH, 64291 Darmstadt, Germany*
[3]*Department of Physics and Helsinki Institute of Physics, University of Helsinki, P.O. Box 64, FI-00014, Finland*
[4]*TUM Physik-Department, Technische Universität München, James-Franck-Str. 1, 85748 Garching, Germany*
[5]*Excellence Cluster ORIGINS, Boltzmannstrasse 2, 85748 Garching, Germany*

(Received 25 July 2023; revised 29 September 2023; accepted 5 October 2023; published 1 November 2023)

Accurately understanding the equation of state (EOS) of high-density, zero-temperature quark matter plays an essential role in constraining the behavior of dense strongly interacting matter inside the cores of neutron stars. In this Letter, we study the weak-coupling expansion of the EOS of cold quark matter and derive the complete, gauge-invariant contributions from the long-wavelength, dynamically screened gluonic sector at next-to-next-to-next-to-leading order (N3LO) in the strong coupling constant α_s. This elevates the EOS result to the $O(\alpha_s^3 \ln \alpha_s)$ level, leaving only one unknown constant from the unscreened sector at N3LO, and places it on par with its high-temperature counterpart from 2003.

DOI: 10.1103/PhysRevLett.131.181902

Introduction.—A proper understanding of the thermodynamics of dense strongly interacting matter is an outstanding problem in theoretical physics. This is in large part due to the infamous sign problem of lattice field theory [1–5], which renders nonperturbative lattice Monte Carlo techniques largely inapplicable in the region of large baryon chemical potential μ_{B} and low temperatures T in quantum chromodynamics (QCD).

At densities above 40 times the nuclear saturation density, $n_0 \approx 0.16\ \mathrm{fm}^{-3}$, a perturbative weak-coupling expansion in the strong coupling constant α_s becomes applicable within the fundamental theory of QCD, due to asymptotic freedom. In this regime, it becomes possible to study the thermodynamics of cold (zero-temperature) quark matter (QM) directly using well-established thermal-field-theory tools [6–9]. The equation of state (EOS) of high-density cold QM has in recent years received increasing attention as a robust high-density constraint [10] to be used when performing neutron-star EOS inference at lower densities [11–27]. In addition to this phenomenological application, there is great theoretical interest to study high-density cold QM, due to the rich physics arising from the dynamical screening of long-wavelength chromoelectric and chromomagnetic fields. These screening effects necessitate the development of an effective field theory of the long-wavelength gluonic modes, which goes beyond a fixed loop order in the weak-coupling expansion.

Such screening also occurs in a high-temperature quark-gluon plasma. However, at high temperatures, low-energy chromoelectric and chromomagnetic gluons can additionally receive large thermal occupation numbers $\sim 1/\alpha_s^{1/2}$ or $\sim 1/\alpha_s$, respectively [28]. These large occupation numbers lead to poor perturbative convergence within the long-wavelength chromoelectric sector of QCD and necessitate a nonperturbative treatment of the chromomagnetic sector at high temperatures. Crucially, however, such a long-wavelength "Bose enhancement" is absent within high-density unpaired cold QM, and hence the thermodynamics of such a system *always* remains a perturbative problem. Furthermore, we also emphasize that this conclusion is not modified by any possible color superconducting phases that may exist at high densities, since the corrections to bulk thermodynamics from these effects are exponentially suppressed $\sim \exp(-\#/\alpha_s^{1/2})$ [29–31].

Since long-wavelength gluons are not Bose enhanced in cold QM, one could, in principle, extend the results for the EOS to even lower densities by tackling increasingly higher-order perturbative computations—something which could lead to dramatic improvements within the aforementioned neutron-star EOS-inference setups. In this Letter, we compute the full EOS contributions from the screened gluonic sector at next-to-next-to-next-to-leading order (N3LO) in α_s in unpaired cold QM, bringing the result to the $O(\alpha_s^3 \ln \alpha_s)$ level and on par with its high-temperature counterpart from 2003 [32]. This is achieved by deriving the next-to-leading order (NLO) screening corrections to long-wavelength gluon propagation in cold QM, generalizing the recent results in [33,34] to zero temperature. We find that our result shows very small renormalization-scale dependence for $\mu_{\rm B}$ where it is convergent, suggesting that the screened gluonic sector is under good perturbative control at high densities.

Structure of the weak-coupling expansion of the EOS.—In the context of cold QM with vanishing quark masses in the grand canonical ensemble, the EOS is given by the free energy density $\Omega = -p$, where p is pressure, as a function of the quark and lepton chemical potentials. In astrophysical environments, the conditions of charge-neutral, three-flavor quark matter in equilibrium under the weak interactions (beta equilibrium) are the most relevant. These conditions reduce the EOS to a function of a single quantity $\mu_{\rm B}$. Up to and including NLO, the EOS, which we henceforth identify as $p(\mu_{\rm B})$, is sensitive only to "hard" quark and gluonic corrections from momenta $K \sim \mu_{\rm B}$, since the low-momentum quarks are Pauli blocked and the screened gluonic sector is phase-space suppressed: $\int_{K<\alpha_s^{1/2}\mu_{\rm B}} d^4K \simeq \alpha_s^2 \mu_{\rm B}^4$. However, beginning at next-to-next-to-leading order (N2LO) in α_s, which was computed in 1977 in the context of cold QM [35,36], the pressure becomes sensitive to long-wavelength, screened gluonic fluctuations. These field modes can be described via the hard thermal loop (HTL) effective theory [28,37] [or hard dense loop (HDL) [38–40]], which captures the physics of the "soft" momentum scale $m_{\rm E} \sim \alpha_s^{1/2}\mu_{\rm B}$, corresponding to chromoelectric screening. At N2LO, because of the phase-space suppression, self-interactions between these screened gluons do not yet contribute. At the next order in α_s, however, interactions involving these screened fluctuations must be included. In particular, there arise contributions from self-interactions among the fluctuating soft modes and also interactions between fluctuating soft and hard modes. The pressure correction arising from the self-interactions at N3LO has been computed within the leading-order HTL theory [41,42], while the pressure correction arising from interactions between the soft and hard modes involves corrections to the leading-order HTL theory. These corrections to high-density HTL have been calculated within QED [43–45] at zero and high temperatures, and recently within QCD [33,34] at high temperatures.

In total therefore, the pressure of cold QM at N3LO can be written in the form

$$p_{\rm N3LO} = p^s + p^m + p^h, \tag{1}$$

where the three terms on the right-hand side come from the different combinations of soft and hard momentum scales. The first term p^s is the purely soft contribution arising from self-interactions between screened gluon field modes. The second term p^m, dubbed the mixed contribution, arises from the corrections within the HTL theory. Finally, in addition to soft and mixed terms, there are also fully hard contributions p^h, entering the expansion via four-loop vacuum graphs in full QCD (see [42] for a list). In this work, we compute the screened correction p^m from the mixed sector.

The screened gluonic modes lead to nonanalyticities in the pressure, arising from logarithms of the ratio of the soft and hard scales $\ln(m_{\rm E}/\mu_{\rm B})$. To N3LO, the pressure p of cold and dense, beta-equilibrated three-color, three-flavor ($N_c = N_f = 3$) unpaired QM with massless quarks can be cast into the following form [36,46–48], (see [49] for the general N_c and N_f expressions)

$$\frac{p}{p_{\rm free}} \simeq 1 - 2\left(\frac{\alpha_s}{\pi}\right) - 3\left(\frac{\alpha_s}{\pi}\right)^2\left[\ln\left(3\frac{\alpha_s}{\pi}\right) + 3\ln X + 5.0021\right] + 9\left(\frac{\alpha_s}{\pi}\right)^3\left[c_{3,2}\ln^2\left(3\frac{\alpha_s}{\pi}\right) + c_{3,1}(X)\ln\left(3\frac{\alpha_s}{\pi}\right) + c_{3,0}(X)\right], \tag{2}$$

where $p_{\rm free} = 3(\mu_{\rm B}/3)^4/4\pi^2$ is the pressure of a free Fermi gas of quarks in beta equilibrium, $\alpha_s = \alpha_s(\bar\Lambda)$ is the renormalized strong coupling constant in the $\overline{\rm MS}$ scheme at the renormalization scale $\bar\Lambda$, and $X \equiv 3\bar\Lambda/(2\mu_{\rm B})$ is a quantity which should be taken to be $O(1)$ to minimize large logarithms. We have written logarithms of α_s by grouping them in the natural expansion parameter $N_f\alpha_s/\pi$, and set $N_f = 3$. The coefficient $c_{3,2}$ of the leading logarithm was originally determined in [48]. Recently, an all-order leading-logarithm resummation was conducted in [52], using this term as input.

In this work, we conclusively determine the coefficient $c_{3,1}(X)$ of the next-to-leading logarithm. It should be emphasized that this term is a well-defined and independent coefficient in the perturbative series. While the coefficient is now fully determined, the parts of the $c_{3,1}(X)$ contribution proportional to $\ln X$ could already be inferred from renormalization group invariance using lower-order results. Likewise, given this newly determined contribution, all parts of $c_{3,0}(X)$ proportional to $\ln^k X$ can now be inferred with similar arguments, thus resulting in the entire $p_{\rm N3LO}$ except for one constant from the hard sector.

Overview of the calculation.—The mixed contributions correspond to the following diagrams stemming from the classification of [42]

$p^m =$

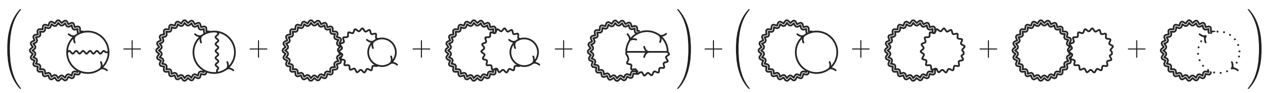

$=$

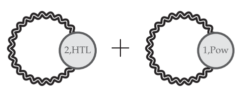

$$= -\frac{\alpha_s m_{\mathrm{E}}^2 d_A}{8\pi} \int_K \mathrm{Tr}\left\{ G_{\mathrm{LO}}(K) \left[\Pi^{2,\mathrm{HTL}}(K) + \frac{K^2}{m_{\mathrm{E}}^2} \Pi^{1,\mathrm{Pow}}(K) \right] \right\}. \tag{3}$$

The double wavy lines correspond to soft, HTL-resummed gluons; the wavy, solid, and dotted lines correspond to hard, unresummed gluons, quarks, and ghosts, respectively; and the trace is over the suppressed Lorentz indices. Furthermore, a sum over the direction of fermionic flow is implied. In Eq. (3), the two shaded blobs and the respective Π's correspond to the two distinct NLO soft gluon self-energies at zero temperature: namely, the two-loop corrections given in the first pair of parentheses and the power corrections, given by the $O(K^2)$ term in a small-K expansion, given in the second. The G_{LO} is the standard one-loop resummed HTL propagator [37,38], $d_A = N_c^2 - 1$, K is the loop momentum associated with the soft gluon, and the Π's have been rescaled to be dimensionless and independent of α_s, (see details and explicit expressions in [49]). In dimensional regularization and in the $\overline{\mathrm{MS}}$ scheme, the integration measure is defined by $\int_K \equiv (e^{\gamma_{\mathrm{E}}} \Lambda_{\mathrm{h}}^2/(4\pi))^{(4-D)/2} \int \mathrm{d}^D K/(2\pi)^D$, where $D \equiv 4 - 2\varepsilon$ and Λ_{h} is the factorization scale associated with the split between the hard and soft modes [42,53]. The complete Feynman rules can be found in [42].

Note that $\Pi^{2,\mathrm{HTL}}$ and $\Pi^{1,\mathrm{Pow}}$ entering in Eq. (3) have been recently computed at high temperature and large μ_{B} in general covariant gauge [33], where they have been shown to contain $\ln T$ terms that diverge in the zero-temperature limit. These terms arise because the temperature regulates certain infrared (IR) divergences associated with the hard internal gluon lines in the self-energy diagrams. The corresponding zero-temperature self-energies are computed in [49] in terms of d-dimensional integral expressions. The zero-temperature limit is achieved by using the exact integral expressions of these self-energies and isolating divergent bosonic integrals that vanish at exactly zero temperature in dimensional regularization. This procedure effectively converts, after renormalization, the $\ln T$ terms into IR $1/\varepsilon$ terms in the strict zero-temperature expressions. We find that the final expressions for the self-energies depend linearly on the gauge parameter ξ in a general covariant gauge, in contrast to the quadratic dependence found at high temperatures in [33].

With the renormalized self-energies in hand, the mixed contribution to the pressure can then be obtained by computing the integral in Eq. (3). The integral over the soft momentum K contains ultraviolet (UV) divergences that arise because the HTL theory differs from full QCD in the UV. These UV divergences must cancel with corresponding IR divergences in the hard theory, contained in p^h. This cancellation has been explicitly shown in QED, where the soft sector trivially vanishes, [53], but due to the added complexity of QCD, we do not show this explicitly—however, the cancellation must occur as long as HTL does indeed correctly describe the soft physics at this order.

Importantly, upon computing the radial K integral in Eq. (3), we find that only the specific combination of self-energies $\Pi^{2,\mathrm{HTL}} - \Pi^{1,\mathrm{HTL}}\Pi^{1,\mathrm{Pow}}$ appears. Here $\Pi^{1,\mathrm{HTL}}$ denotes the standard one-loop HTL self-energy [37,38], appearing in G_{LO}. This particular combination is explicitly gauge-invariant, guaranteeing the gauge invariance of the mixed contribution to the pressure. We remark here that this should be the case since the 2-loop HTL pressure corresponding to the soft sector is known to be gauge independent [42,54], and the 4-loop hard-sector diagrams are likewise known to be algebraically gauge invariant [55]. We note also that the above self-energy combination also naturally appears when one rescales the HTL effective Lagrangian including the 2-loop and power corrections to bring the kinetic term to a canonical form [34,56].

Results and discussion.—Upon computing the renormalized p^m in dimensional regularization (details are given in [49], in general N_c and N_f), we find it to have a similar form to the p^s computed in [41,42], namely,

$$p^m = \frac{\alpha_s m_{\mathrm{E}}^4 d_A}{(4\pi)^3} \left(\frac{m_{\mathrm{E}}}{\Lambda_{\mathrm{h}}} \right)^{-2\varepsilon} \left(\frac{\mu_{\mathrm{B}}/3}{\Lambda_{\mathrm{h}}} \right)^{-2\varepsilon} \times \left(\frac{p_{-2}^m}{(2\varepsilon)^2} + \frac{p_{-1}^m(X)}{2\varepsilon} + p_0^m(X) \right), \tag{4}$$

where the coefficients p_i^m denote terms in the ε expansion and do not depend on the coupling. The factor $(m_{\mathrm{E}}/\Lambda_{\mathrm{h}})^{-2\varepsilon}$ arises from the integral over the soft-theory loop momentum K in Eq. (3), while the factor $[\mu_{\mathrm{B}}/(3\Lambda_{\mathrm{h}})]^{-2\varepsilon}$ arises from the hard-theory calculation leading to the self-energies. We find the new coefficients p_i^m in Eq. (4) to be

$$p_{-2}^m = -11; \qquad p_{-1}^m(X) = 9 \ln X - 4.8095,$$
$$p_0^m(X) = -\frac{9}{2} \ln^2 X + 2.0598 \ln X - 5.6316. \tag{5}$$

TABLE I. List of numerical values for the coefficients appearing in Eq. (2).

$c_{3,2}$	$11/12$
$c_{3,1}$	$-6.5968(12) - 3\ln X$
$c_{3,0}$	$5.1342(48) + \frac{2}{3}c_0 - 18.284\ln X - \frac{9}{2}\ln^2 X$

We note that this now confirms through an explicit calculation a prediction made in [42]: $p^m_{-2} = -2p^s_{-2}$.

We then combine this result with similar expressions for p^s and p^h in Eq. (1) (whose expressions are given in [49]) and obtain the renormalized result for the full N3LO pressure

$$p_{\mathrm{N3LO}} = \frac{\alpha_s m_{\mathrm{E}}^4 d_A}{(4\pi)^3}\left[p^s_{-2}\ln^2\left(\frac{\mu_{\mathrm{B}}/3}{m_{\mathrm{E}}}\right) + \left(2p^s_{-1} + p^m_{-1}(X)\right) \times \ln\left(\frac{\mu_{\mathrm{B}}/3}{m_{\mathrm{E}}}\right) + p^s_0 + p^m_0(X) + p^h_0(X)\right]. \qquad (6)$$

As mentioned above, we here assume the intermediate IR and UV divergences between the different sectors to fully cancel, which in turn ensures that the Λ_{h} dependence from the different sectors cancels. From renormalization-scale independence of the partial result (see, e.g., [53]), we are additionally able to determine the full X dependence of p^h_0(X), leading to the form

$$p^h_0(X) = -\frac{9}{4}\ln^2 X - 26.367\ln X + c_0. \qquad (7)$$

Equations (4)–(7) are our main result, and they fix the coefficients in the pressure in Eq. (2) to be those given in Table I, with c_0 the remaining unknown constant from the hard sector.

In Fig. 1 we show the partial N3LO pressure, neglecting only the finite hard contribution $p^h_0(X)$ at this order. In the figure, the uncertainty of the truncation of the perturbative series is estimated by varying of $X \in [1/2, 2]$, shown as a shaded uncertainty band. In this and all subsequent figures, we use the three-loop beta function when computing the running $\alpha_s(\bar{\Lambda})$. We see from Fig. 1 that the pressure contribution when including the screened gluonic sector at N3LO is remarkably well converged. In particular, it has nearly vanishing renormalization-scale dependence for all $\mu_{\mathrm{B}} > 2$ GeV. In fact, we have verified that one obtains a similarly well-converged result when neglecting the hard contribution at N2LO as well. This is consistent with the observation made in [41,42]: In cold QM, it is the hard terms $p^h(X)$ that drive the inevitable breakdown of perturbation theory, in stark contrast to the high-temperature case where the soft modes are responsible for the breakdown.

We turn now to an analysis of the full N3LO pressure, which we have now determined up to a single unknown

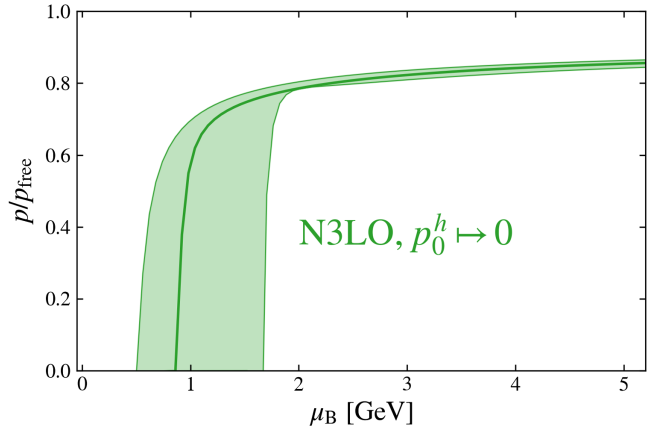

FIG. 1. The N3LO pressure normalized by the free pressure as a function of baryon chemical potential, including all contributions but the hard contributions $p^h_0(X)$ in Eq. (7). The shaded region shows the usual scale variation of $X \in [1/2, 2]$, while the solid line is the central scale choice $X = 1$.

constant from the hard sector c_0. Upon substituting in different values, we find that the N3LO pressure strongly depends on c_0. An approximate value for this constant can only be determined by computing many hard four-loop diagrams—a project which will take several years of effort. Hence, we are motivated to find an alternative way to estimate its value in order to quantify how well converged we may expect the full N3LO result to be.

Since the perturbative series for the pressure of cold QM is well-behaved up to N2LO, we turn to a Bayesian model to identify which values of c_0 are most consistent with lower-order results [57]. In particular, we use the *abc* model of convergent series as presented in [58] and implemented in the publicly available `MiHO` code [59]. This Bayesian model, as well as the geometric model from [60] was recently applied to the high-density perturbative-QCD EOS in [61]. These models assume that the perturbative series can be approximated by independent draws from a statistical model of convergent series. Upon conditioning these models using the NLO and N2LO results using Bayes's theorem, they provide posterior distributions for the N3LO pressure as a function of μ_{B} and X, quantifying the degree to which a given p_{N3LO} is consistent with the lower-order results. We choose to perform the following analysis at a fixed $\mu_{\mathrm{B}} = 2.6$ GeV, which is the canonical value down to which the N2LO results are typically used [11]. We have checked that our conclusions remain similar if we choose a slightly different matching μ_{B} (see also [61]).

As the N3LO pressure is now a function of a single parameter c_0, posterior distributions of p_{N3LO} at fixed X can be converted to distributions of c_0. To combine the resulting c_0 distributions for different X values, we choose to marginalize over the fictitious renormalization parameter $X \in [1/2, 2]$ following the procedure introduced in [60].

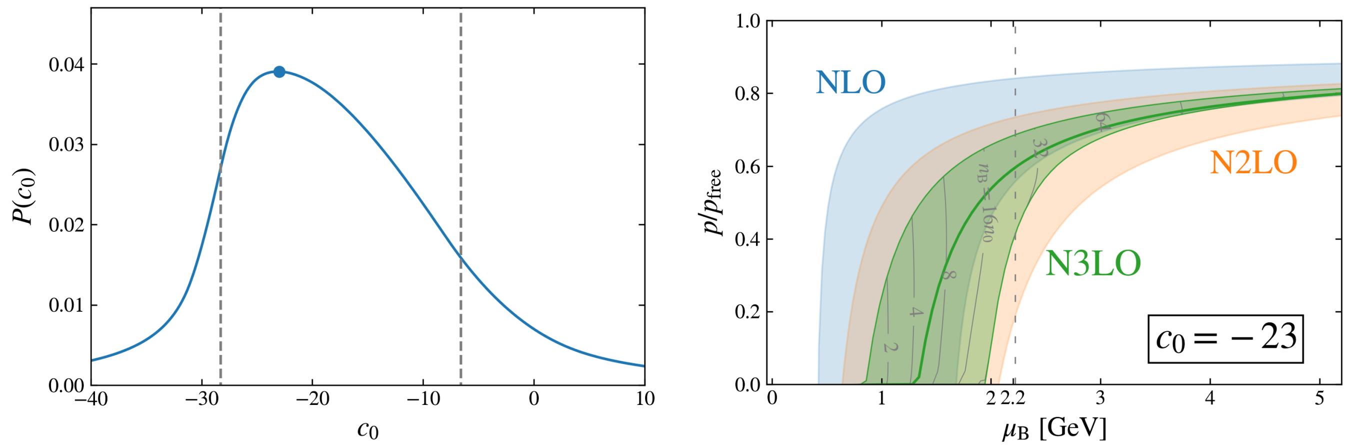

FIG. 2. (Left) The posterior distribution of c_0 within the *abc* model after marginalizing over $X \in [1/2, 2]$ [58] at $\mu_{\mathrm{B}} = 2.6$ GeV (see main text). The dashed lines correspond to the 68% credible interval, and the solid point is the maximum of the distribution. (Right) The resulting N3LO pressure for most-consistent value $c_0 = -23$. The dashed line at $\mu_{\mathrm{B}} = 2.2$ GeV denotes the point where the N3LO result possesses $\pm 25\%$ errors, and the gray lines denote contours of constant number density.

This marginalization weights different values of the renormalization parameter in proportion to how well the *abc* model is converged at that X. This results in larger values of X receiving slightly larger weights, and furthermore leads to a slightly more conservative distribution than would result from the alternative scale-averaging procedure [58] in this case.

The above analysis leads to the probability distribution $P(c_0)$ shown in the left panel of Fig. 2. The distribution is rather broad, with a 68% credible interval corresponding to $c_0 \in [-29, -6]$, denoted in Fig. 2 by the dashed gray lines. We find that the distribution takes its highest value at $c_0 = -23$, denoted by the blue point in this figure. The resulting N3LO pressure corresponding to this most-consistent value of c_0 is shown in the right panel of Fig. 2, where the shaded region denotes the standard scale variation of $X \in [1/2, 2]$. We find that for this value, the full N3LO pressure of cold QM lies inside the N2LO result and is well converged. In particular, the errors reach $\pm 25\%$ at $\mu_{\mathrm{B}} = 2.2$ GeV, corresponding to about $n = 27n_0$, denoted in the right panel of this figure by the dashed gray line. This is to be contracted with $n \approx 40n_0$ for the N2LO result at $\mu_{\mathrm{B}} = 2.6$ GeV. We note that between these densities, the relative importance of the pairing contribution to the pressure increases only by ~ 2, so pairing effects do not grow appreciably. We thus see as an outcome of this Bayesian modeling that significant improvement to the cold-QM EOS may occur by computing the remainder of the N3LO pressure.

Conclusions.—In this Letter, we have fully computed the contributions from the screened gluonic sector at next-to-next-to-next-to leading order in the strong coupling α_s. This elevates the perturbative-QCD equation of state of cold quark matter to the $O(\alpha_s^3 \ln \alpha_s)$ level, leaving only one constant from the hard sector left to be computed, and finally places it on par with its high-temperature counterpart. We have achieved this by deriving the next-to-leading-order corrections to soft gluon propagation within a high-density medium, extending existing hard-thermal-loop results to the zero-temperature limit.

A natural follow-up to this work is the evaluation of the remaining hard constant. This would allow for the use of the full N3LO equation of state in applications, such as in studies of the neutron-star-matter equation of state. As this is an involved undertaking, it will require the development of new tools and methods. Some work in this direction has already been performed [62–64] and more is ongoing.

We thank Aleksi Kurkela, Aleksas Mazeliauskas, and Aleksi Vuorinen for their helpful comments and suggestions. This work is supported in part by the Deutsche Forschungsgemeinschaft (DFG, German Research Foundation)–Project ID 279384907–SFB 1245 and by the State of Hesse within the Research Cluster ELEMENTS (Project ID 500/10.006) (T. G.). R. P. and K. S. have been supported by the Academy of Finland Grants No. 347499 and No. 353772 as well as by the European Research Council, Grant No. 725369. S. S. acknowledges support of the DFG cluster of excellence ORIGINS funded by the DFG under Germany's Excellence Strategy—EXC-2094-390783311. In addition, K. S. gratefully acknowledges support from the Finnish Cultural Foundation.

[*]tyler.gorda@physik.uni-frankfurt.de
[†]risto.paatelainen@helsinki.fi
[‡]saga.saeppi@tum.de
[§]kaapo.seppanen@helsinki.fi

[1] P. Hasenfratz and F. Karsch, Chemical potential on the lattice, Phys. Lett. **125B**, 308 (1983).

[2] J. B. Kogut, H. Matsuoka, M. Stone, H. W. Wyld, S. H. Shenker, J. Shigemitsu, and D. K. Sinclair, Chiral symmetry restoration in baryon rich environments, Nucl. Phys. **B225**, 93 (1983).

[3] F. Karsch and H. W. Wyld, Complex Langevin Simulation of the SU(3) spin model with nonzero chemical potential, Phys. Rev. Lett. **55**, 2242 (1985).

[4] P. de Forcrand, Simulating QCD at finite density, Proc. Sci. LAT2009 (**2009**) 010.

[5] K. Nagata, Finite-density lattice QCD and sign problem: Current status and open problems, Prog. Part. Nucl. Phys. **127**, 103991 (2022).

[6] J. I. Kapusta and C. Gale, *Finite-Temperature Field Theory: Principles and Applications*, Cambridge Monographs on Mathematical Physics (Cambridge University Press, Cambridge, England, 2011), 10.1017/CBO9780511535130.

[7] M. Le Bellac, *Thermal Field Theory*, Cambridge Monographs on Mathematical Physics (Cambridge University Press, Cambridge, England, 2011), 10.1017/CBO9780511721700.

[8] M. Laine and A. Vuorinen, *Basics of Thermal Field Theory* (Springer, New York, 2016), Vol. 925, 10.1007/978-3-319-31933-9.

[9] J. Ghiglieri, A. Kurkela, M. Strickland, and A. Vuorinen, Perturbative thermal QCD: Formalism and applications, Phys. Rep. **880**, 1 (2020).

[10] O. Komoltsev and A. Kurkela, How perturbative QCD constrains the equation of state at neutron-star densities, Phys. Rev. Lett. **128**, 202701 (2022).

[11] A. Kurkela, E. S. Fraga, J. Schaffner-Bielich, and A. Vuorinen, Constraining neutron star matter with Quantum Chromodynamics, Astrophys. J. **789**, 127 (2014).

[12] E. Annala, T. Gorda, A. Kurkela, and A. Vuorinen, Gravitational-wave constraints on the neutron-star-matter equation of state, Phys. Rev. Lett. **120**, 172703 (2018).

[13] E. R. Most, L. R. Weih, L. Rezzolla, and J. Schaffner-Bielich, New constraints on radii and tidal deformabilities of neutron stars from GW170817, Phys. Rev. Lett. **120**, 261103 (2018).

[14] S. Altiparmak, C. Ecker, and L. Rezzolla, On the sound speed in neutron stars, Astrophys. J. Lett. **939**, L34 (2022).

[15] E. Annala, T. Gorda, A. Kurkela, J. Nättilä, and A. Vuorinen, Evidence for quark-matter cores in massive neutron stars, Nat. Phys. **16**, 907 (2020).

[16] E. Annala, T. Gorda, E. Katerini, A. Kurkela, J. Nättilä, V. Paschalidis, and A. Vuorinen, Multimessenger constraints for ultradense matter, Phys. Rev. X **12**, 011058 (2022).

[17] T. Gorda, O. Komoltsev, and A. Kurkela, Ab-initio QCD calculations impact the inference of the neutron-star-matter equation of state, Astrophys. J. **950**, 107 (2023).

[18] R. Somasundaram, I. Tews, and J. Margueron, Perturbative QCD and the neutron star equation of state, Phys. Rev. C **107**, L052801 (2023).

[19] J.-L. Jiang, C. Ecker, and L. Rezzolla, Bayesian analysis of neutron-star properties with parameterized equations of state: The role of the likelihood functions, Astrophys. J. **949**, 11 (2023).

[20] Y. Fujimoto, K. Fukushima, L. D. McLerran, and M. Praszalowicz, Trace anomaly as signature of conformality in neutron stars, Phys. Rev. Lett. **129**, 252702 (2022).

[21] M. Marczenko, L. McLerran, K. Redlich, and C. Sasaki, Reaching percolation and conformal limits in neutron stars, Phys. Rev. C **107**, 025802 (2023).

[22] T. Gorda, K. Hebeler, A. Kurkela, A. Schwenk, and A. Vuorinen, Constraints on strong phase transitions in neutron stars, Astrophys. J. **955**, 100 (2023).

[23] A. Sorensen *et al.*, Dense nuclear matter equation of state from heavy-ion collisions, arXiv:2301.13253.

[24] J. Takatsy, P. Kovacs, G. Wolf, and J. Schaffner-Bielich, What neutron stars tell about the hadron-quark phase transition: A Bayesian study, Phys. Rev. D **108**, 043002 (2023).

[25] R. Essick, I. Legred, K. Chatziioannou, S. Han, and P. Landry, Phase transition phenomenology with nonparametric representations of the neutron star equation of state, Phys. Rev. D **108**, 043013 (2023).

[26] L. Brandes, W. Weise, and N. Kaiser, Evidence against a first-order phase transition in neutron star cores: Impact of new data, arXiv:2306.06218.

[27] D. Mroczek, M. C. Miller, J. Noronha-Hostler, and N. Yunes, Nontrivial features in the speed of sound inside neutron stars, arXiv:2309.02345.

[28] J.-P. Blaizot and E. Iancu, The quark gluon plasma: Collective dynamics and hard thermal loops, Phys. Rep. **359**, 355 (2002).

[29] D. T. Son, Superconductivity by long range color magnetic interaction in high density quark matter, Phys. Rev. D **59**, 094019 (1999).

[30] H. Malekzadeh and D. H. Rischke, Gluon self-energy in the color-flavor-locked phase, Phys. Rev. D **73**, 114006 (2006).

[31] M. G. Alford, A. Schmitt, K. Rajagopal, and T. Schäfer, Color superconductivity in dense quark matter, Rev. Mod. Phys. **80**, 1455 (2008).

[32] K. Kajantie, M. Laine, K. Rummukainen, and Y. Schroder, The pressure of hot QCD up to g6 ln(1/g), Phys. Rev. D **67**, 105008 (2003).

[33] T. Gorda, R. Paatelainen, S. Säppi, and K. Seppänen, Soft gluon self-energy at finite temperature and density: hard NLO corrections in general covariant gauge, J. High Energy Phys. 08 (2023) 021.

[34] A. Ekstedt, Propagation of gauge fields in hot and dense plasmas at higher orders, arXiv:2304.09255.

[35] B. A. Freedman and L. D. McLerran, Fermions and gauge vector mesons at finite temperature and density. 2. The ground state energy of a relativistic electron gas, Phys. Rev. D **16**, 1147 (1977).

[36] B. A. Freedman and L. D. McLerran, Fermions and gauge vector mesons at finite temperature and density. 3. The ground state energy of a relativistic quark gas, Phys. Rev. D **16**, 1169 (1977).

[37] E. Braaten and R. D. Pisarski, Soft amplitudes in hot gauge theories: A general analysis, Nucl. Phys. **B337**, 569 (1990).

[38] C. Manuel, Hard dense loops in a cold nonAbelian plasma, Phys. Rev. D **53**, 5866 (1996).

[39] A. Ipp, A. Gerhold, and A. Rebhan, Anomalous specific heat in high density QED and QCD, Phys. Rev. D **69**, 011901(R) (2004).

[40] A. Ipp, K. Kajantie, A. Rebhan, and A. Vuorinen, The pressure of deconfined QCD for all temperatures and quark chemical potentials, Phys. Rev. D **74**, 045016 (2006).

[41] T. Gorda, A. Kurkela, R. Paatelainen, S. Säppi, and A. Vuorinen, Soft interactions in cold quark matter, Phys. Rev. Lett. **127**, 162003 (2021).
[42] T. Gorda, A. Kurkela, R. Paatelainen, S. Säppi, and A. Vuorinen, Cold quark matter at N3LO: Soft contributions, Phys. Rev. D **104**, 074015 (2021).
[43] S. Carignano, C. Manuel, and J. Soto, Power corrections to the HTL effective Lagrangian of QED, Phys. Lett. B **780**, 308 (2018).
[44] S. Carignano, M. E. Carrington, and J. Soto, The HTL Lagrangian at NLO: The photon case, Phys. Lett. B **801**, 135193 (2020).
[45] T. Gorda, A. Kurkela, J. Österman, R. Paatelainen, S. Säppi, P. Schicho, K. Seppänen, and A. Vuorinen, Soft photon propagation in a hot and dense medium to next-to-leading order, Phys. Rev. D **107**, 036012 (2023).
[46] G. Baym and S. A. Chin, Landau theory of relativistic fermi liquids, Nucl. Phys. **A262**, 527 (1976).
[47] G. Chapline, Jr. and M. Nauenberg, Phase transition from baryon to quark matter, Nature (London) **264**, 235 (1976).
[48] T. Gorda, A. Kurkela, P. Romatschke, S. Säppi, and A. Vuorinen, Next-to-next-to-next-to-leading order pressure of cold quark matter: Leading logarithm, Phys. Rev. Lett. **121**, 202701 (2018).
[49] See Supplemental Material at http://link.aps.org/supplemental/10.1103/PhysRevLett.131.181902 for additional details of the self-energy and pressure computations, which includes Refs. [50,51].
[50] M. Laine and Y. Schroder, Two-loop QCD gauge coupling at high temperatures, J. High Energy Phys. 03 (2005) 067.
[51] A. Vuorinen, The pressure of QCD at finite temperatures and chemical potentials, Phys. Rev. D **68**, 054017 (2003).
[52] L. Fernandez and J.-L. Kneur, All order resummed leading and next-to-leading soft modes of dense QCD pressure, Phys. Rev. Lett. **129**, 212001 (2022).
[53] T. Gorda, A. Kurkela, J. Österman, R. Paatelainen, S. Säppi, P. Schicho, K. Seppänen, and A. Vuorinen, Degenerate fermionic matter at N3LO: Quantum electrodynamics, Phys. Rev. D **107**, L031501 (2023).
[54] J. O. Andersen, E. Braaten, E. Petitgirard, and M. Strickland, HTL perturbation theory to two loops, Phys. Rev. D **66**, 085016 (2002).
[55] Y. Schroder, Automatic reduction of four loop bubbles, Nucl. Phys. B, Proc. Suppl. **116**, 402 (2003).
[56] K. Kajantie, M. Laine, K. Rummukainen, and M. E. Shaposhnikov, Generic rules for high temperature dimensional reduction and their application to the standard model, Nucl. Phys. **B458**, 90 (1996).
[57] M. Cacciari and N. Houdeau, Meaningful characterisation of perturbative theoretical uncertainties, J. High Energy Phys. 09 (2011) 039.
[58] C. Duhr, A. Huss, A. Mazeliauskas, and R. Szafron, An analysis of Bayesian estimates for missing higher orders in perturbative calculations, J. High Energy Phys. 09 (2021) 122.
[59] Alexander Huss, miho (2021), https://github.com/aykhuss/miho.
[60] M. Bonvini, Probabilistic definition of the perturbative theoretical uncertainty from missing higher orders, Eur. Phys. J. C **80**, 989 (2020).
[61] T. Gorda, O. Komoltsev, A. Kurkela, and A. Mazeliauskas, Bayesian uncertainty quantification of perturbative QCD input to the neutron-star equation of state, J. High Energy Phys. 06 (2023) 002.
[62] I. Ghisoiu, T. Gorda, A. Kurkela, P. Romatschke, S. Säppi, and A. Vuorinen, On high-order perturbative calculations at finite density, Nucl. Phys. **B915**, 102 (2017).
[63] T. Gorda, J. Österman, and S. Säppi, Augmenting the residue theorem with boundary terms in finite-density calculations, Phys. Rev. D **106**, 105026 (2022).
[64] J. Österman, P. Schicho, and A. Vuorinen, Integrating by parts at finite density, J. High Energy Phys. 08 (2023) 212.